J|A|C|S
ARTICLES
Published on Web 05/23/2002

# Heme Charge-Transfer Band III Is Vibronically Coupled to the Soret Band

Stefan Franzen,* Stacie E. Wallace-Williams, and Andrew P. Shreve

*Contribution from the Department of Chemistry, North Carolina State University, Raleigh, North Carolina 27695, and Bioscience Division, Los Alamos National Laboratory, Los Alamos, New Mexico 87545*

Received October 9, 2001

***Abstract:*** A complete resonance Raman excitation profile of the heme charge-transfer band known as band III is presented. The data obtained throughout the near-infrared region show preresonance with the Q-band, but the data also clearly show the enhancement of a number of modes in the spectral region of band III. Only nontotally symmetric modes are observed to have resonance enhancement in the band III region. The observed resonance enhancements in modes of $B_{1g}$ symmetry are compared with the enhancements of those same modes in the excitation profiles of the Q-band of deoxy myoglobin, also presented here for this first time. The Q-band data agree well with the theory of vibronic coupling in metalloporphyrins (Shelnutt, J. A. *J. Chem. Phys.* **1981**, *74*, 6644−6657). The strong vibronic coupling of the Q-band of the deoxy form of hemes is discussed in terms of the enhancement of modes with both $B_{1g}$ and $A_{2g}$ symmetry. The comparison between the Q-band and band III reveals that, consistent with the theory, only modes of $B_{1g}$ symmetry are enhanced in the vicinity of band III. These results show that band III is vibronically coupled to the Soret band. The coupling of band III to modes with strong rhombic distortion of the heme macrocycle calls into question the hypothesis that the axial iron out-of-plane displacement is primarily responsible for the structure-dynamics correlations observed in myoglobin.

## Introduction

Spectroscopic studies of proteins play the important role of bridging the gap between structure and dynamics. Because time-dependent changes in protein structure are crucial for their function, these studies also play a key role in connecting structure and function. The protein dynamics of myoglobin have been studied exhaustively by spectroscopy, and although we are nearing a complete picture of the dynamics, important issues remain. In this study, we show that one of the central observables in spectroscopic studies of myoglobin, a small absorption band known as band III centered at 762 nm, is allowed by means of vibronic coupling, and not by a Franck−Condon mechanism. This result changes the interpretation of a large number of studies on myoglobin and impacts the models that connect structure and dynamics. These results are relevant because of the large number of time-dependent studies using both infrared spectroscopy and time-resolved X-ray crystallography that combine to create a detailed picture of myoglobin dynamics following ligand photolysis.

The time-dependent frequency shift of band III has become one of the important observations in myoglobin. Studies of the time-dependence and temperature-dependence of spectral shifts in band III have led to a detailed picture of the sequence of events that follows photolysis of CO. The data have been interpreted in terms of conformational changes in photolyzed carbonmonoxymyoglobin (MbCO).[2−21] Following ligand pho-

* To whom correspondence should be addressed. E-mail: Stefan_Franzen@ncsu.edu.

(1) Shelnutt, J. A. *J. Chem. Phys.* **1981**, *74*, 6644−6657.
(2) Stavrov, S. S. *Chem. Phys.* **2001**, *271*, 145−154.
(3) Jackson, T. A.; Lim, M.; Anfinrud, P. A. *Chem. Phys.* **1994**, *180*, 131−140.
(4) Lim, M.; Jackson, T. A.; Anfinrud, P. A. *Proc. Natl. Acad. Sci. U.S.A.* **1993**, *90*, 5801−5804.
(5) Lambright, D. G.; Balasubramanian, S.; Boxer, S. G. *Chem. Phys.* **1991**, *158*, 249−260.
(6) Lambright, D. G.; Balasubramanian, S.; Boxer, S. G. *Biochemistry* **1993**, *32*, 10116−10124.
(7) Ansari, A.; Jones, C. M.; Henry, E. R.; Hofrichter, J.; Eaton, W. A. *Science* **1992**, *256*, 1796−1798.
(8) Ansari, A.; Jones, C. M.; Henry, E. R.; Hofrichter, J.; Eaton, W. A. *Biochemistry* **1994**, *33*, 5128−5145.
(9) Steinbach, P. J.; Ansari, A.; Berendzen, J.; Braunstein, D.; Chu, K.; Cowen, B. R.; Ehrenstein, D.; Frauenfelder, H.; Johnson, J. B.; Lamb, D. C.; Luck, S.; Mourant, J. R.; Nienhaus, G. U.; Ormos, P.; Philipp, R.; Xie, A.; Young, R. D. *Biochemistry* **1991**, *30*, 3988−4001.
(10) Nienhaus, G. U.; Mourant, J. R.; Frauenfelder, H. *Proc. Natl. Acad. Sci. U.S.A.* **1992**, *89*, 2902−2906.
(11) Srajer, V.; Reinisch, L.; Champion, P. M. *J. Am. Chem. Soc.* **1988**, *110*, 6656−6670.
(12) Srajer, V.; Champion, P. M. *Biochemistry* **1991**, *30*, 7390−7402.
(13) Tian, W. D.; Sage, J. T.; Srajer, V.; Champion, P. M. *Phys. Rev. Lett.* **1992**, *68*, 408−411.
(14) Ahmed, A. M.; Campbell, B. F.; Caruso, D.; Chance, M. R.; Chavez, M. D.; Courtney, S. H.; Friedman, J. M.; Iben, I. E. T.; Ondrias, M. R.; Yang, M. *Chem. Phys.* **1991**, *158*, 329−351.
(15) Chavez, M. D.; Courtney, S. H.; Chance, M. R.; Kuila, D.; Nocek, J.; Hoffman, B. M.; Friedman, J. M.; Ondrias, M. R. *Biochemistry* **1990**, *29*, 4844−4852.
(16) Kiger, L.; Stetzkowski-Marden, F.; Poyart, C.; Marden, M. *Eur. J. Biochem.* **1995**, *228*, 665−668.
(17) Gilch, H.; SchweitzerStenner, R.; Dreybrodt, W.; Leone, M.; Cupane, A.; Cordone, L. *Int. J. Quantum Chem.* **1996**, *59*, 301−313.
(18) Franzen, S.; Boxer, S. G. *J. Biol. Chem.* **1997**, *272*, 9655−9660.
(19) Galkin, O.; Buchter, S.; Tabirian, A.; A, S. *Biophys. J.* **1997**, *73*, 2752−2763.
(20) Huang, J.; Ridsdale, A.; Wang, J. Q.; Friedman, J. M. *Biochemistry* **1997**, *36*, 14353−14365.
(21) Ormos, P.; Szaraz, S.; Cupane, A.; Nienhaus, G. U. *Proc. Natl. Acad. Sci. U.S.A.* **1998**, *95*, 6762−6767.


**10.1021/ja0172722 CCC: $22.00** 

tolysis in MbCO, the absorption maxima of both the Soret band and the charge-transfer band III of the heme are observed shifted to 140 $cm^{-1}$ lower energy in the photoproduct Mb*CO than in the equilibrium spectrum for deoxy myoglobin. At cryogenic temperatures, the Mb*CO photoproduct spectra do not relax from their initial 140 $cm^{-1}$ shifted position.[9,12,14,22] However, above the glass transition temperature (160−170 K), there is a time-dependent shift of the Soret and band III maxima from their initial shifted position, indicating that structural coordinates in the protein responsible for the band III shift can relax under these conditions. The time-dependent shift reflects rapid structural relaxations that precede CO ligand rebinding and is highly nonexponential even at room temperature in nonviscous solutions where geminate CO rebinding is single exponential.[3,4] One of the remarkable attributes of the observed band shifts is that the Soret band and band III behave similarly, although the Soret band is the most intense $\pi-\pi^*$ band in the absorption spectrum, and band III is a very weak charge-transfer transition.[23]

In fact, the central importance of band III for the understanding of the complex set of phenomena is surprising. To provide some background, band III rivals band IV as the smallest detectable heme absorption band in the deoxy Mb spectrum. At its maximum wavelength of 762 nm, the extinction coefficient is $\epsilon \approx 200$ $M^{-1}$ $cm^{-1}$.[23] Band III is more than 1000 times less intense than the Soret band. Although the Soret band in deoxy myoglobin has an inhomogeneous broadening of 400 $cm^{-1}$, the apparent inhomogeneous broadening band III is only 25 $cm^{-1}$. [12] Although band III has been assigned as a charge-transfer band, it is quite narrow, and models that fit the line shape find only weak coupling to a Franck−Condon low-frequency mode.[12] Band III exhibits anomalous temperature dependence.[12] As the temperature is lowered from 300 to 10 K, band III increases in intensity without changing either its bandwidth or $\lambda_{max}$. The MCD spectrum of band III is not A-term, as would be expected on the basis of the assignment as a $a_{2u}(\text{ring}) \rightarrow e_g(d_\pi)$ transition. The B-term MCD signal implies symmetry breaking leading to the assignment of band III as a $a_{2u}(\text{ring}) \rightarrow e_g(d_{yz})$ transition.[23]

There has been a great deal of theoretical study of the structural origin of the protein relaxation that gives rise to the observed band shift. Here, a phenomenon known as kinetic hole-burning has played an important role. At temperatures below 20 K, CO recombines very slowly by tunneling.[24] Following photolysis at temperatures below 20 K, band III appears (shifted by 140 $cm^{-1}$ from the equilibrium value as discussed above).[12,25] If CO is then allowed to partially recombine (e.g., at $T > 40$ K), the intensity is reduced on the low energy side of band III instead of uniformly across the band. These results indicate a correlation between the frequency of the band III electronic transition and the barrier to CO ligand rebinding.[12,20,21] A number of groups have suggested that the origin of the structural change sensed by band III is the iron out-of-plane position.[3,7,9,12] This model is based on the assignment of band III as a charge-transfer band[23] along with the assumption that the spectral position of band III is related to the iron out-of-plane position. This assumption reflects that the energy of the charge-transfer band is thought to depend on iron position because of the resulting change in overlap of the iron $d\pi$ orbitals with the $e_g$ $\pi^*$ orbitals of the porphyrin ring. Although deoxy heme is best represented by $C_{4v}$ symmetry at the iron, we retain the $D_{4h}$ nomenclature for the porphyrin-centered states to be consistent with a large body of literature. On the basis of the magnetic circular dichroism (MCD) data, band III is assigned as a transition from $a_{2u}(\pi\text{-ring}) \rightarrow d_{yz}$, one of two d orbitals of $\pi$ symmetry (overall symmetry of $E_u$ for the excited state).[23] The fact that the excited state of band III involves only one of the two possible $d_\pi$ orbitals ($d_{xz}$ and $d_{yz}$) indicates symmetry breaking.

However, models in the literature have not considered the role of the nontotally symmetric vibrations.[26] These may vibronically couple band III to the Soret band and give rise to a means for environmental effects to change the energy of heme electronic transitions by a different mechanism than axial out-of-plane displacement of the heme iron. Vibronic coupling is known for similar charge-transfer bands in ferric heme and in a range of metalloporphyrins that has been studied by resonance Raman spectroscopy.[27,28]

In a previous study of band III, we observed that the difference dipole moment between the ground and excited state is significantly smaller than expected for a charge-transfer band.[29] Also, the angle $\zeta_A$ between the transition moment and the difference dipole is large. In contrast, band I, which does behave as a charge-transfer band, has a difference dipole $\Delta\mu_A = 3.5$ D and an angle $\zeta_A \approx 20°$.[29] On the basis of these observations, we hypothesized that the Raman excitation profile would address the assignment and character of the transition.

The current study presents the first resonance Raman excitation profile of band III and demonstrates that several high-frequency and one prominent low-frequency nontotally symmetric modes are vibronically active. This study differs from previous work on the resonance Raman of band III in that we present a complete resonance Raman excitation profile (REP) that demonstrates the vibronic nature of band III.[26] The coupling of nontotally symmetric modes to both band III and the Soret band, and the absence of coupling of totally symmetric modes to band III, suggest that the totally symmetric axial iron out-of-plane displacement is not responsible for the band shifts of the Soret band and band III. It is proposed instead that the spectral shifts can arise primarily from distal conformational changes to accommodate the photolyzed ligand and nonaxial displacement of the iron and histidine that distort the symmetry of the heme.

## Experimental Section

Horse heart myoglobin (HHMb) was obtained from Sigma. Solutions of 10 mM HHMb were prepared in 10 mM phosphate buffer (pH 7.0). The aqueous solutions were centrifuged to remove any undissolved

(22) Cupane, A.; Vitrano, E.; Ormos, P.; Nienhaus, G. U. *Biophys. J.* **1996**, *60*, 111−117.
(23) Eaton, W. A.; Hanson, L. K.; Stephens, P. J.; Sutherland, J. C.; Dunn, J. B. R. *J. Am. Chem. Soc.* **1978**, *100*, 4991−5003.
(24) Alben, J. O.; Beece, D.; Bowne, S. F.; Eisenstein, L.; Frauenfelder, H.; Good, D.; Marden, M. C.; Moh, P. P.; Reinisch, L.; Reynolds, A. H.; Yue, K. T. *Phys. Rev. Lett.* **1980**, *44*, 1157−1160.
(25) Ansari, A.; Berendzen, J.; Braunstein, D.; Cowen, B. R.; Frauenfelder, H.; Hong, M. K.; Iben, I. E. T.; Johnson, J. B.; Ormos, P.; Sauke, T. B.; Scholl, R.; Schulte, A.; Steinbach, P. J.; Vittitow, J.; Young, R. D. *Biophys. Chem.* **1987**, *26*, 337−355.
(26) Palaniappan, V.; Bocian, D. F. *J. Am. Chem. Soc.* **1994**, *116*, 8839−8840.
(27) Koboyashi, H.; Shimizu, M.; Fujita, I. *Bull. Chem. Soc. Jpn.* **1970**, *43*, 2335−2341.
(28) Shelnutt, J. A.; O'Shea, D. C.; Yu, N.-T.; Cheung, L. D.; Felton, R. H. *J. Chem. Phys.* **1976**, *64*, 1156−1165.
(29) Franzen, S.; Moore, L. J.; Woodruff, W. H.; Boxer, S. G. *J. Am. Chem. Soc.* **1999**, *121*, 3070−3072.

protein. The deoxy ferrous form of myoglobin was prepared by dilution of the concentrated 10 mM stock solution into deoxygenated buffer followed by reduction with a small excess of sodium dithionite. Samples in aqueous phosphate buffer solution at pH 7.0 were studied (5−10 mM concentration) as well as samples prepared in 50% glycerol/buffer solution (5 mM concentration). For experiments at ambient temperature, buffered deoxy HHMb solutions were placed in a spinning NMR tube. Experiments at 40 K were carried out in an Air Products liquid helium cooled refrigerator. The temperature was monitored by a calibrated gold-constantan thermocouple in intimate contact with the coldfinger. The Raman excitation laser was focused on a sample contained in a depression in the coldfinger at the tip of the expander unit.

Near-infrared Raman spectra were obtained with a SpectraPhysics Argon ion laser pumped SpectraPhysics 3090 Ti:sapphire laser operating between 700 and 920 nm. The scattered Raman light was collected using lenses and dispersed using a SPEX 1807 triple monochromator/spectrograph using a 100 $\mu$m slit width, and then detected using a liquid-nitrogen cooled Princeton Instruments CCD camera. Typical laser powers were 50 mW, and accumulation times ranged from 1 to 6 h per spectrum for near-infrared excitation. A separate Raman spectrometer was used for the visible resonance Raman experiments. The visible lines of a Coherent Innova 400 argon ion laser were used to pump a Coherent 590 dye laser (Rhodamine 6G dye) to provide excitation wavelengths between 560 and 620 nm. In addition, argon ion lines at 514.5, 501, and 488 nm were used, as was the quasi-cw 532 nm output of a Coherent Antares 76S modelocked Nd:YAG laser. Scattered light was collected by f/1 5 cm focal length lens and focused on the slit of a SPEX 1807. Slit widths were set to 50 $\mu$m to provide a 2.5 $cm^{-1}$ resolution on a Photometrics CCD camera. Accumulation times were 20 min for the visible spectra. Both the dye laser and the Ti:sapphire laser are tunable so that shifted excitation Raman difference spectra could be obtained.[32,33] These spectra consisted of a Raman data acquisition at a particular excitation frequency followed by an acquisition at a frequency shifted +10 $cm^{-1}$. The two spectra are then subtracted. This technique permits the detection of small Raman peaks on a fluorescent background and is useful for determining the presence of genuine Raman peaks when the signals are very small.

## Results

Deoxy myoglobin samples in the Displex refrigerator at 40 K were studied by resonance Raman using laser excitation wavelengths in the near-infrared between 710 and 850 nm. As the excitation frequency approaches 710 nm, there is a noticeable fluorescent background. On the basis of studies using visible excitation wavelengths, we established that this fluorescence is due to intrinsic fluorescence of the Q-band, and is peaked at 680 nm (see below). As the excitation wavelength is tuned closer to resonance with band III at 762 nm, the fluorescence decreased, and by 800 nm there was no trace of fluorescent background in the data.

Raman spectra of myoglobin in frozen glycerol/buffer solution at 40 K for excitation wavelengths of 740, 760, 767, 773, and 780 nm are presented in Figure 1. The glycerol/buffer (solvent) spectrum is the bottom spectrum in Figure 1. The glycerol peak at 1463 $cm^{-1}$ served as an internal standard in the high-frequency region. Similarly, the ice peak at 229 $cm^{-1}$ and a glycerol peak at 675 $cm^{-1}$ were used to determine relative

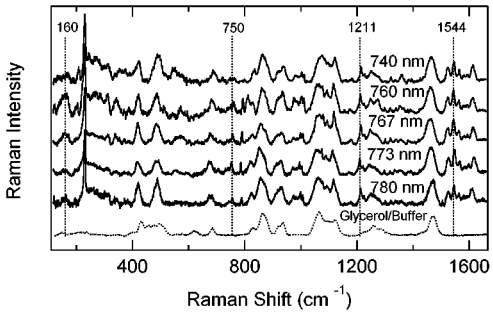


***Figure 1.*** Raman spectra of deoxy heme in myoglobin at 40 K with near-infrared laser excitation are shown. The Raman spectra from 100 to 1700 $cm^{-1}$ are shown for five excitation wavelengths (from the top spectrum) 740, 760, 767, 773, and 780 nm. A 50% (w/w) glycerol/buffer control experiment is shown in the bottom spectrum with excitation at 750 nm. Four modes that are resonantly enhanced in the region of band III are indicated by dotted lines in the figure.

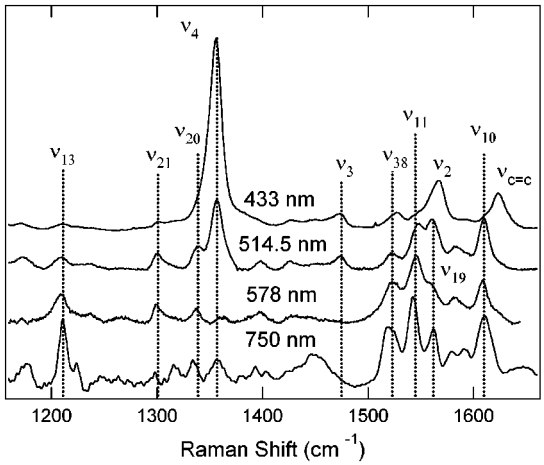


***Figure 2.*** Resonance Raman spectra in resonance with the Soret, Q-band, and band III are shown. The excitation wavelengths shown are 433 nm (Soret resonance), 514.5 nm (Soret and Q-band), 578 nm (Q-band), and 750 nm. The 750 nm spectrum shows that nontotally symmetric modes are present in the Raman spectrum in near-infrared region.

resonance Raman scattering cross sections of the low-frequency modes. Although there are no prominent Raman bands in the glycerol/buffer spectrum below 400 $cm^{-1}$, there are ice peaks evident between 229 and 305 $cm^{-1}$ in the deoxy myoglobin solution spectra, consistent with observations that have been made in Soret resonant Raman spectra at cryogenic temperature.[30,31] The weight percentage of glycerol is 50% in both the glycerol/buffer blank (bottom spectrum) and the deoxy myoglobin samples. Analysis of the data shown in Figure 1 shows that, relative to the solvent features, modes at 160, 750, 1211, and 1544 $cm^{-1}$ are enhanced at 760, 767, and 773 nm (see below and Figure 5).

A comparison of high-frequency Raman spectra obtained with excitation wavelengths in resonance with the Soret absorption band (433 nm), the Q-band (578 nm), and the near-infrared region near band III (750 nm) is shown in Figure 2. The near-infrared Raman spectra more closely resemble Q-band spectra than Soret band spectra. The Raman bands enhanced in resonance with the Soret band are principally Franck−Condon active totally symmetric modes ($A_{1g}$ modes in the $D_{4h}$ point group), although there are also less intense $B_{1g}$ and $A_{2g}$ modes that are enhanced by intrastate vibronic coupling.[1] Figure 2 shows that the onset of resonance with the Q-band (514.5 nm

(30) Ondrias, M. R.; Rousseau, D. L.; Simon, S. R. *Proc. Natl. Acad. Sci. U.S.A.* **1982**, *79*, 1511−1514.
(31) Ondrias, M. R.; Rousseau, D. L.; Simon, S. R. *J. Biol. Chem.* **1983**, *258*, 5638−5642.
(32) Shreve, A.; Cherepy, N.; Franzen, S.; Boxer, S. G.; Mathies, R. A. *Proc. Natl. Acad. Sci. U.S.A.* **1991**, *88*, 11207−11211.
(33) Shreve, A. P.; Cherepy, N. J.; Mathies, R. A. *Appl. Spectrosc.* **1992**, *46*, 707−711.

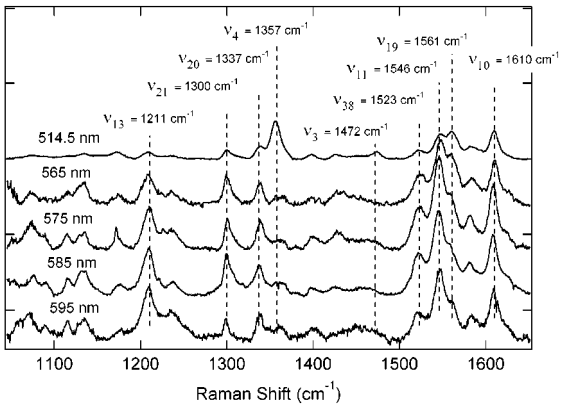


***Figure 3.*** Raman spectra obtained for excitation at various wavelengths in resonance with the Q-band. All of the assigned Raman bands indicated in the figure are attributable to nontotally symmetric modes except for $\nu_3$ and $\nu_4$, which are only observed in the 514.5 nm spectrum and gain intensity through the Soret band resonance. Modes with numbers from $\nu_{10}-\nu_{18}$ are $B_{1g}$ modes. Modes with numbers from $\nu_{19}-\nu_{28}$ are $A_{2g}$ modes. The mode $\nu_{38}$ is an $E_u$ mode that normally would be observed only in the infrared spectrum. Because of symmetry lowering, this mode is often observed in the resonant Raman spectrum.

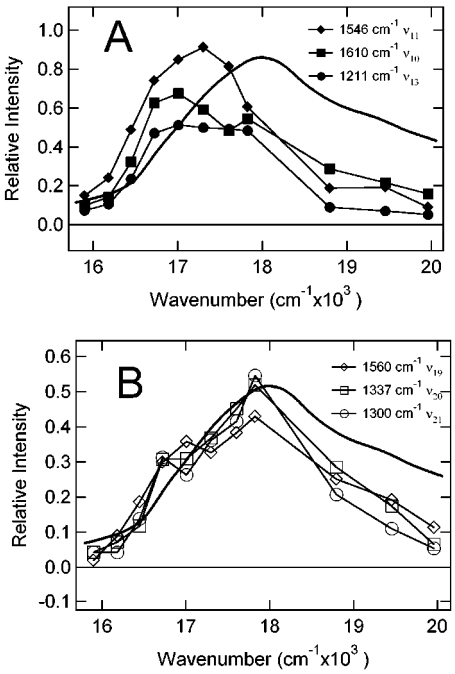


***Figure 4.*** The Raman excitation profiles for laser excitation in resonance with Q-band of deoxy myoglobin are shown. (A) REPs for three modes of $B_{1g}$ symmetry are shown ($\nu_{10}$, $\nu_{11}$, and $\nu_{13}$). (B) REPs for three modes of $A_{2g}$ symmetry are shown ($\nu_{19}$, $\nu_{20}$, and $\nu_{21}$).

excitation) coincides with enhancement of a number of nontotally symmetric modes, the $B_{1g}$ modes $\nu_{10}$, $\nu_{11}$, and $\nu_{13}$, the $A_{2g}$ modes $\nu_{19}$, $\nu_{20}$, and $\nu_{21}$, and the $E_u$ mode $\nu_{38}$ (Table 1). These modes gain intensity as laser excitation is tuned through resonance with the Q-band. It is important to consider the Q-band resonance Raman spectrum since many of the observed modes seen at 750 nm may gain intensity through preresonant excitation of the Q-band.

For comparison with band III spectra, we consider resonant Q-band excitation shown in Figure 3 to determine the symmetries and REPs of Raman active modes. Excitation from 501 to 630 nm was used to obtain a complete Raman excitation

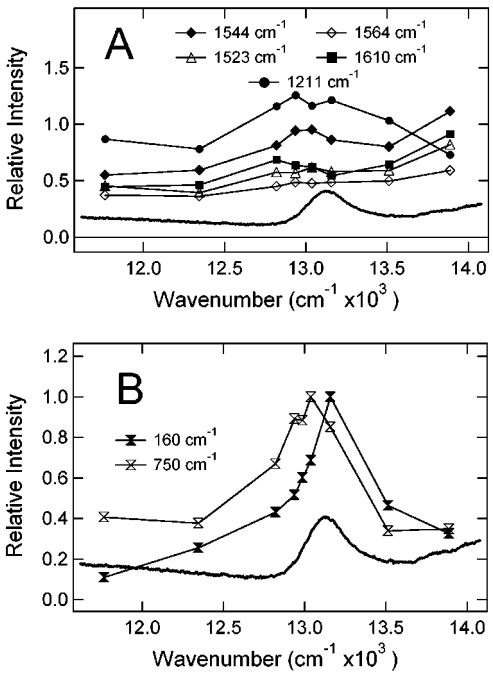


***Figure 5.*** Raman excitation profiles (REPs) for both high- (A) and low- (B) frequency modes in the near-infrared spectral region. (A) The REPs for several high-frequency modes are shown. The absorption spectrum of band III obtained at 80 K is shown as the solid trace in the figure. The modes shown are $\nu_{13}$ (1211 $cm^{-1}$), $\nu_{11}$ (1544 $cm^{-1}$), $\nu_{38}$ (1523 $cm^{-1}$), $\nu_{19}$ (1564 $cm^{-1}$). Enhancement is seen for $B_{1g}$ modes $\nu_{11}$ and $\nu_{13}$, but not other modes. (B) The REPs for two low-frequency modes of $B_{1g}$ symmetry are shown. The 750 $cm^{-1}$ mode has been assigned as $\nu_{15}$. The 160 $cm^{-1}$ mode has not been assigned.

***Table 1.*** Table of Depolarization Ratios for Raman Active Modes Observed with 514.5 nm Laser Excitation

| frequency | $\rho$ (514.5 nm) | assignment | irreducible representation |
|---|---|---|---|
| 1172 | 0.424 | $\nu_{30}$ | $E_u$ |
| 1211 | 0.332 | $\nu_{13}$ | $B_{1g}$ |
| 1233 | 0.483 | $\delta_S(=CH_2)$ | NA |
| 1301 | 1.410 (ap) | $\nu_{21}$ | $A_{2g}$ |
| 1339 | 0.767 (ap) | $\nu_{20}$ | $A_{2g}$ |
| 1356 | 0.373 (p) | $\nu_4$ | $A_{1g}$ |
| 1395 | 0.636 | $\nu_{29}$ | $E_u$ |
| 1427 | 0.651 | $\delta_S(=CH_2)$ | NA |
| 1475 | 0.243 (p) | $\nu_3$ | $A_{1g}$ |
| 1522 | 0.608 | $\nu_{38}$ | $E_u$ |
| 1546 | 0.808 | $\nu_{11}$ | $B_{1g}$ |
| 1562 | 1.000 (ap) | $\nu_{19}$ | $A_{2g}$ |
| 1585 | 0.519 | $\nu_{37}$ | $E_u$ |
| 1610 | 0.470 | $\nu_{10}$ | $B_{1g}$ |

profile of the Q-band. The fluorescent background began to interfere strongly with Raman spectra for wavelengths longer than 590 nm. To obtain spectra on the fluorescent background, the technique of shifted excitation Raman difference spectroscopy was applied throughout the Q-band as a check of relative Raman intensities (data not shown).[32,33] The low-frequency region of the Q-band shows less intense bands at 160, 370, 674, and 750 $cm^{-1}$ for 514 nm excitation and no bands below 750 $cm^{-1}$ for 585 nm excitation (data not shown). The REPs of prominent high-frequency vibrational modes are shown in Figure 4. As a check on the symmetry of assigned modes, depolarization ratios were determined at 514.5 and 585 nm (Table 1).

The REPs of modes of $B_{1g}$ symmetry are shown in Figure 4A, and those of $A_{2g}$ symmetry are shown in Figure 4B. The

modes of $A_{2g}$ symmetry all have smaller 0−0 transitions than 0−1 transitions, while the opposite is true for modes of $B_{1g}$ symmetry. In fact, the $B_{1g}$ modes show the greatest resonance Raman enhancement in a region of the absorption spectrum that has very little intensity. The shapes of the REPs for the $A_{2g}$ and $B_{1g}$ modes are in accord with vibronic coupling theory.[1] Calculated models of the REPs and absorption spectra are included in the Supporting Information.

Preresonant Q-band enhancement of nontotally symmetric modes is expected in the near-infrared region. There is significant absorbance in the near-infrared region out to 1100 nm. The bands in this region have been attributed to the tail of the Q-band and to a very broad d−d transition known as band II, as well as charge-transfer bands I, III, and IV. Direct evidence for Raman enhancement in resonance with band II is not available. Band I is at 1000 nm, and Raman spectra for excitation into this band have not been observed. Band IV is a very weak band near 660 nm. For experimental reasons, the band IV region is a very difficult region of the spectrum to probe. These reasons are that Q-band fluorescence, which peaks near 680 nm, obscures any Raman features in this region, and, in addition, band IV is significantly less intense than band III. The preresonant Q-band Raman spectra should decrease monotonically throughout the spectral region of 690−850 nm probed in this study. The spectra shown in Figure 1 were analyzed to ascertain whether bands showed an increase in intensity in the region near 762 nm, the maximum of band III.

In the vicinity of band III, there are enhancements of the nontotally symmetric modes indicated in Figure 1. The enhancement is not only evident relative to an external standard, but also among several of the high-frequency modes themselves (see the Supporting Information). The symmetry requirements for vibronic coupling of a $a_{2u} \rightarrow d_{yz}$ charge-transfer band with the Soret band (or Q-band) require vibronic activity from only $B_{1g}$ or $B_{2g}$ modes and not $A_{2g}$ modes.[28] However, there are no intense Raman-active $B_{2g}$ modes observed in the Q-band spectra nor enhanced in resonance with band III, so modes of $B_{2g}$ symmetry are not considered further. Consistent with vibronic theory,[28] the only modes with REPs showing resonance enhancement from band III have $B_{1g}$ symmetry. Figure 5A shows REPs for several high-frequency modes. Of these, only the 1211 and 1544 $cm^{-1}$ mode, which have been assigned to the $\nu_{13}$ and $\nu_{11}$ $B_{1g}$ vibrational modes, respectively, demonstrate enhancement in the band III region. As seen in the spectra in Figures 2 and 3 and REPs in Figure 4A, $B_{1g}$ modes are also enhanced in resonance with the Q-band.

Examination of the low-frequency region of band III resonant Raman spectra is considerably more difficult. In addition to glycerol bands, there are ice bands even in a 50% glycerol buffer glass sample. However, these bands can also be used as internal standards to create a relative REP. Raman bands at 160, 345, 750, and 785 $cm^{-1}$ are attributable to deoxy heme, as distinct from the solvent bands. However, the 345 and 785 $cm^{-1}$ bands are not clearly observed in room-temperature shifted excitation Raman difference spectra. The origin of the 345 and 785 $cm^{-1}$ modes is discussed further in the Supporting Information, and these modes are not considered further in the analysis.

The REPs of modes at 160 and 750 $cm^{-1}$ observed in resonance with band III are shown in Figure 5B. The 750 $cm^{-1}$ band is a prominent band in the Raman spectrum of the Soret band (e.g., with excitation at 433 nm). The 750 $cm^{-1}$ band has been assigned as $\nu_{15}$.[34] The 160 $cm^{-1}$ Raman band observed in Raman spectra at 40 K can be identified with the 150 $cm^{-1}$ band observed in Soret Raman spectra at ambient temperature. The depolarization ratio of the 150 $cm^{-1}$ band is 0.4 in Raman spectra obtained in resonance with the Soret band.[35] This depolarization ratio is indicative of a mode of $B_{1g}$ symmetry, and such an assignment is consistent with the observation of a number of other modes of $B_{1g}$ symmetry in the Soret resonance Raman spectrum (e.g., $\nu_{11}$, $\nu_{13}$, and $\nu_{15}$). The 160 $cm^{-1}$ band observed here is quite broad, suggesting the presence of two bands. This appearance is similar to the 150 $cm^{-1}$ band observed in resonance with Soret band, which also appears to consist of two bands.[35] The origin of the discrepancy of 10 $cm^{-1}$ in the frequency is likely due to the temperature difference in the two measurements. It is well known that the Fe−His mode shifts by nearly 10 $cm^{-1}$ to higher wavenumber as the temperature is lowered from ambient temperature to 10 K.[17,31] Although it has not been observed directly in temperature-dependent Soret resonance Raman spectra, the 150 $cm^{-1}$ mode is expected to undergo a similar shift. The origin of the shift could be conformational strain or anharmonic coupling to low-frequency out-of-plane modes.[36]

The 150 $cm^{-1}$ band observed in the Soret resonance Raman spectrum is sensitive to axial ligation as observed in resonance Raman spectra of the myoglobin mutant H93G with various ligands to the heme iron in the proximal cavity.[37] Specifically, the 150 $cm^{-1}$ band is much reduced in intensity when $H_2O$ is the axial ligand.[38] On the basis of the intensity dependence of this mode on axial ligand replacements, we have concluded that the 160 $cm^{-1}$ band has out-of-plane character.[37] Therefore, the assignment of this mode is a rhombic distortion of the pyrrole nitrogens combined with some out-of-plane character. It is possible that the 160 $cm^{-1}$ mode has similarities with $\nu_{18}$, the lowest-frequency $B_{1g}$ mode predicted in a $D_{4h}$ analysis of metalloporphines. In $C_{4v}$ symmetry, the distinction between $B_{1g}$ (in-plane) and $B_{1u}$ (out-of-plane) symmetry is lost, and this would simply be a $B_1$ mode. The nature of the 160 $cm^{-1}$ mode and the origin of its Soret band resonance enhancement due to intrastate vibronic coupling are discussed below.

Room-temperature experiments are important to corroborate the conclusions based on the 40 K spectra. One disadvantage of 40 K spectra is the presence of the ice Raman band at 229 $cm^{-1}$, which is close enough to potentially interfere with the signal at 218 $cm^{-1}$, the frequency of the iron-histidine band. However, experiments under ambient conditions did not provide a route to obtain better REPs. Deoxy myoglobin samples were distinctly less stable in buffer solution at room temperature. Experimentation for less than 1 h resulted in a significant increase in fluorescence. The fluorescent background was worse when cosolvents glycerol or ethylene glycol were added or when

(34) Hu, S.; Smith, K. M.; Spiro, T. G. *J. Am. Chem. Soc.* **1996**, *118*, 12638−12646.
(35) Bangcharoenpaurpong, O.; Schomaker, K. T.; Champion, P. M. *J. Am. Chem. Soc.* **1984**, *106*, 5688−5698.
(36) Rosenfeld, Y. B.; Stavrov, S. S. *Chem. Phys. Lett.* **1994**, *229*, 457−464.
(37) Franzen, S.; Boxer, S. G.; Dyer, R. B.; Woodruff, W. H. *J. Phys. Chem. B* **2000**, *104*, 10359−10367.
(38) Franzen, S.; Bailey, J.; Dyer, R. B.; Woodruff, W. H.; Hu, R. B.; Thomas, M. R.; Boxer, S. G. *Biochemistry* **2001**, *40*, 5299−5305.

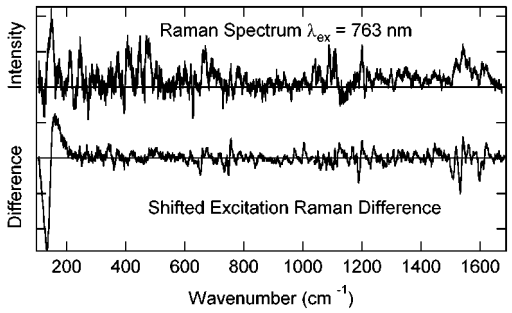


***Figure 6.*** Near-infrared deoxy myoglobin Raman spectra obtained at room temperature. The top spectrum is baseline corrected by subtraction of a spine fit to the baseline of the data. The bottom spectrum is a shifted excitation Raman difference spectrum obtained by taking the difference between the Raman spectrum obtained with laser excitation at 13 090 $cm^{-1}$ and a second spectrum obtained using 13 080 $cm^{-1}$ excitation.

$Na_2SO_4$ was added as an internal standard. In addition, resonance Raman scattering was observed to be less intense at room temperature, consistent with the fact that the extinction coefficient of band III is lower by nearly a factor of 2 at 300 K than it is at 40 K.

Despite these difficulties, both the Raman spectrum and the shifted excitation Raman difference spectrum were obtained under room-temperature conditions and are shown in Figure 6. Although a number of Raman bands appear in the low-frequency region at room temperature, many of these bands are not observed in the shifted excitation Raman difference spectrum. The reason for this is that the Raman bands are observed as small features on a large sloping baseline at room temperature. The spectrum shown in Figure 6 has been corrected by baseline subtraction. For a sufficiently large background, the subtraction of the baseline can easily lead to artifacts. The shifted excitation Raman difference spectrum does verify the key vibrations that are observed in the low-temperature work. The mode at 1211 $cm^{-1}$ ($\nu_{13}$) is prominent, as are the modes at 1523 $cm^{-1}$ ($\nu_{38}$), 1544 $cm^{-1}$ ($\nu_{11}$), 1610 $cm^{-1}$ ($\nu_{10}$), and 750 $cm^{-1}$ ($\nu_{15}$). The spectral region of the 160 $cm^{-1}$ band is obscured by a Rayleigh artifact that was observed even in pure buffer spectra. One important result is that there is no feature near 218 $cm^{-1}$ in the shifted excitation difference spectrum shown in the bottom trace of Figure 6. Thus, the data in Figure 6 indicate that there is no large enhancement of the iron-histidine out-of-plane mode,[39−41] and in this regard the room-temperature experiments corroborate the 40 K data in that only $B_{1g}$ vibrational modes are observed.

## Discussion

Near-infrared laser excitation of deoxy heme at 40 K yields resonant Raman spectra of band III that show enhancement of nontotally symmetric vibrational modes of $B_{1g}$ symmetry. The shifted excitation technique was applied both at room temperature and at low temperature to show Raman features that are identifiable as nontotally symmetric modes. The modes at 160, 750, 1211, and 1544 $cm^{-1}$ that are resonantly enhanced in the 40 K spectra were not observed in a previous report of room-temperature band III spectra.[26] The origin of the difference is likely in the application of a shifted excitation technique in the present study and the fact that the majority of spectra in our study were obtained at 40 K. The data presented here show that room-temperature experiments yield much smaller signals consistent with the smaller extinction coefficient of band III. Without application of the shifted excitation technique, it is difficult to extract the Raman active modes from the room-temperature spectrum due to the level of background.

The observation in this study of nontotally symmetric vibronically active modes resonantly enhanced in band III, though perhaps surprising, is consistent with symmetry-based considerations. In our discussion, we distinguish between totally symmetric modes that show displacements of equilibrium positions upon excitation and nontotally symmetric modes that promote or enhance an electronic transition by lowering the symmetry of a molecule. Specifically, we reserve the term vibronic coupling for the latter, while the former are referred to as Franck−Condon active modes. In heme spectroscopy, there are four mode symmetries that can be coupled to the B and Q $\pi-\pi^*$ transitions based on the four orbital model.[46] Using the $D_{4h}$ point group, as is widely done even for porphyrins with symmetries lower than $D_{4h}$, the in-plane vibrational modes that are coupled to the electronic transitions are the Franck−Condon or totally symmetric $A_{1g}$ modes and the vibronic or nontotally symmetric $B_{1g}$, $B_{2g}$, and $A_{2g}$ modes. Indeed, vibronic coupling involving the latter modes is responsible for the intensity of the Q-band according to theory. The assignment of band III as an $a_{2u} \rightarrow d_{yz}$ transition implies that the excited-state configuration has the same symmetry as those of the B and Q-bands; hence, modes of the same symmetries can vibronically couple band III to the Soret band as well. The observed $B_{1g}$ modes enhanced in resonance with band III are known from either the Soret spectrum[35] or the Q-band spectrum (Figures 2 and 3) and have been assigned in these resonant Raman spectra based on REPs and depolarization ratios.[43,44] Vibronic coupling in the Soret band gives rise to intensity for vibrational modes of $B_{1g}$ symmetry at 750 $cm^{-1}$ ($\nu_{15}$), 1610 $cm^{-1}$ ($\nu_{10}$), and 1544 $cm^{-1}$ ($\nu_{11}$) due to both intrastate (Jahn−Teller) and interstate (Herzberg−Teller) vibronic coupling.[45] In addition, a strong mode at 150 $cm^{-1}$ is observed for Soret band excitation.[34,35] The depolarization ratio of this mode is consistent with a nontotally symmetric mode that is likely to be of $B_{1g}$ character on the basis of theory[1] and the fact that all of the other nontotally symmetric modes observed for Soret band excitation are of $B_{1g}$ symmetry. Interstate vibronic coupling in the Q-band gives rise to intensity in bands at 1610 $cm^{-1}$ ($\nu_{10}$), 1544 $cm^{-1}$ ($\nu_{11}$), and 1211 $cm^{-1}$ ($\nu_{13}$). Prior to the present work, it could have been assumed that the low-frequency $B_{1g}$ modes such as 750 $cm^{-1}$ ($\nu_{15}$) and 160 $cm^{-1}$ owed their intensity to intrastate Jahn−Teller coupling. However, the REPs for band III shown in Figure 5A and B indicate that low-frequency $B_{1g}$ modes are resonantly enhanced by band III excitation and the vibronic

(39) Hori, H.; Kitagawa, T. *J. Am. Chem. Soc.* **1980**, *102*, 3608−3613.
(40) Argade, P. V.; Sassaroli, M.; Rousseau, D. L.; Inubushi, T.; Ikeda-Saito, M.; Lapidot, A. *J. Am. Chem. Soc.* **1984**, *106*, 6593−6596.
(41) Wells, A. V.; Sage, T. J.; Morikis, D.; Champion, P. M.; Chiu, M. L.; Sligar, S. G. *J. Am. Chem. Soc.* **1991**, *113*, 9655−9660.
(42) Engler, N.; Ostermann, A.; Gassmann, A.; Lamb, D. C.; Prusakov, V. E.; Schott, J.; Schweitzer-Stenner, R.; Parak, F. G. *Biophys. J.* **2000**, *78*, 2081−2092.
(43) Li, X. Y.; Czernuszewicz, R. S.; Kincaid, J. R.; Stein, P.; Spiro, T. G. *J. Phys. Chem.* **1990**, *94*, 47−61.
(44) Li, X. Y.; Czernuszewicz, R. S.; Kincaid, J. R.; Su, Y. O.; Spiro, T. G. *J. Phys. Chem.* **1990**, *94*, 31−47.
(45) Shelnutt, J. A.; Cheung, L. D.; Chang, R. C. C.; Yu, N. T.; Felton, R. H. *J. Chem. Phys.* **1977**, *66*, 3387−3396.
(46) Gouterman, M. *J. Chem. Phys.* **1959**, *30*, 1139−1160.

intensity of these modes arises due to vibronic coupling to the Soret band. The nature of vibronic coupling of band III with the Soret band is best understood by comparison with the Q-band.

There is a significant difference between the Q-band and band III with regard to vibronic activity. The four orbital model of metalloporphyrins predicts that modes of $A_{2g}$, $B_{1g}$, and $B_{2g}$ symmetry will vibronically mix the Soret and Q-bands given that these bands arise from the zero order states of $E_u$ symmetry that involve configuration interaction among $^2(a_{1u})^1(a_{2u})^1(e_{gx})$-$(e_{gy})$ and $^1(a_{1u})^2(a_{2u})(e_{gx})^1(e_{gy})$ for *y*-polarized transitions and $^2(a_{1u})^1(a_{2u})(e_{gx})^1(e_{gy})$ and $^1(a_{1u})^2(a_{2u})^1(e_{gx})(e_{gy})$ for *x*-polarized transitions.[46,47] By contrast, only modes of $B_{1g}$ and $B_{2g}$, and *not* $A_{2g}$, symmetry are predicted to give rise to mixing of the CT configurations with the $\pi-\pi^*$ configuration.[28] Thus, one major difference between band III (CT) enhancement and Q-band enhancement ($\pi-\pi^*$) should be the presence of $A_{2g}$ modes in the latter, but not in the former. This theoretical prediction is in agreement with experiment.

A second important difference between the Q and band III vibronic coupling lies in the different character and frequency of the modes that will give rise to strong vibronic coupling. High-frequency modes of the heme macrocycle couple the Q-band to the Soret band. This is observed in the REPs in Figures 4 and 5. Both the $B_{1g}$ and the $A_{2g}$ REPs show clearly that the 0−0 transition for the Q-band is at ~16 950 $cm^{-1}$ (590 nm). Magnetic circular dichroism (MCD) spectra also support this assignment of the 0−0.[48] However, there is little absorbance at the frequency of the 0−0 transition. The maximum in the Q-band absorbance is at 555 nm, approximately 1130 $cm^{-1}$ above the 0−0 transition. There is a second vibronic band at 19 300 $cm^{-1}$, that is, 2350 $cm^{-1}$ above the 0−0 transition. It is apparent that vibronic coupling due to high-frequency modes is very strong in the Q-band of deoxy heme. By contrast, low-frequency modes involving the rhombic distortion of the iron coordination sphere, that is, a $B_{1g}$ symmetry distortion, couple band III to the Soret band. Indeed, there is weak enhancement of high-frequency $B_{1g}$ modes in resonance with band III, but strong coupling to the low-frequency modes. The fact that these modes also gain intensity in the resonance with Soret band is indicative of vibronic coupling of the Soret band to band III.

The fact that interstate Herzberg−Teller coupling exists both for band III and for the Q-band does not rule out a contribution by Jahn−Teller coupling.[45] Indeed, the splitting of the d$\pi$ orbitals of band III is indicated by the B-term MCD signal for this band.[23] Recent study of the C-term MCD signal of the deoxy Soret band substantiates a significant splitting in the Soret band as well.[48−50] A picture of such splitting is shown in Figure 7 where a degenerate excited-state potential surface is split by nuclear motion along a symmetry breaking normal coordinate. The Raman data indicate that the relevant normal mode for excited intrastate coupling is the lowest-frequency $B_{1g}$ mode, which corresponds to the 150 $cm^{-1}$ mode in Soret resonant Raman spectra.

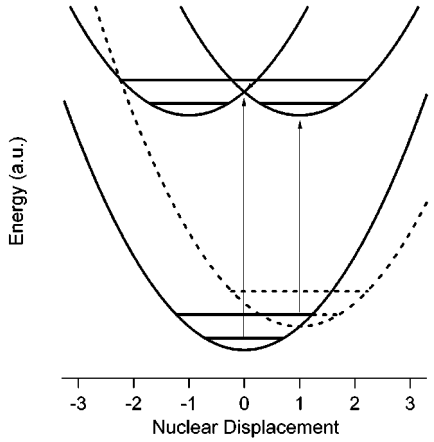


***Figure 7.*** A schematic illustration is presented of how optical transition energies can be affected by Jahn−Teller coupling. The excited state shows two energy minima representing the dependence of the energy on the geometry of a particular nontotally symmetric vibrational normal mode. The excited-state energy is 2-fold degenerate at the point $Q = 0$, which corresponds to a fully symmetric molecule. For an undistorted molecule, the classical vertical electronic transition occurs to the degeneracy point (central arrow). The excited-state symmetry is then lowered by motion along the coordinate shown. In contrast, if the molecule is distorted in the ground state, the vertical transition energy can be moved to lower values, as shown by the right arrow. Subsequent energy stabilization of the ground state could lead to time-dependent changes in the transition energy. The ground-state distortion is only represented schematically, but could occur through environmental perturbations associated with ligand photolysis.

If potential energy surfaces along a nontotally symmetric mode were considered for a simple case lacking degeneracies (no Jahn−Teller activity) or coupling that leads to frequency changes between the ground and excited electronic states, then the vertical transition energy would be independent of position. In other words, the ground- and excited-state potential energy surfaces along this mode would be identical save for a vertical offset. However, given Jahn−Teller activity as pictured schematically in Figure 7, then clearly the vertical transition energy becomes dependent on the coordinate position. If a perturbation leads to a distortion of the ground-state geometry, then a shifting of the vertical transition energy to lower values can result. Further, the magnitude of that shift will be related to the frequency of the Jahn−Teller active mode. Because of symmetry breaking and state-mixing, the transition dipole strength is also dependent on coordinate, and is often expressed in a Taylor series expansion about the undistorted symmetric geometry ($Q = 0$). Both the changes in the potential energy surfaces and the coordinate dependence of the transition dipoles form a basis for resonance Raman activity. Thus, Jahn−Teller coupling leads to Raman enhancement of $B_{1g}$ modes, a splitting of $E_u$ symmetry excited states (based on $e_g\pi^*$ or $d_\pi$ orbitals), and possible band shifts due to geometric distortions of the heme along the Jahn−Teller active mode. These observations have implications for the origin of band shifts in both band III and in the Soret band, as discussed below.

The strong intrastate coupling in band III indicates that the observed transition is either the 0−0 or the 0−1 band. This coupling and the band III line shape are quite different from the predominately interstate coupling of the Q-band that leads to an extensive vibronic progression in the latter. Normally, vibronic coupling would indicate a vibronic progression with a 0−1 band being dominant as observed in the Q-band of deoxy

(47) Zerner, M.; Gouterman, M.; Kobayashi, H. *Theor. Chim. Acta* **1966**, *6*, 363−400.
(48) Franzen, S. *J. Phys. Chem.*, submitted.
(49) Sutherland, J. C.; Axelrod, D.; Klein, M. P. *J. Chem. Phys.* **1971**, *54*, 2888−2898.
(50) Treu, J. I.; Hopfield, J. J. *J. Chem. Phys.* **1975**, *63*, 613−623.

heme. Given that the strongest vibronic mode is the 160 $cm^{-1}$ mode, it is possible that the true origin of band III is 160 $cm^{-1}$ to lower energy and that the observed transition is the 0−1 band. It is difficult to distinguish between these possibilities experimentally.

We consider a vibronic model that explains the intensity of band III. On the basis of the assumptions of the Gouterman four orbital model,[46] we can model the absorption bands and REPs of both the Q-band and the band III transitions on the basis of the pure 50/50 mixing of the $E_u$ excited-state configurations:

$$|B_y^0\rangle = \frac{1}{\sqrt{2}}(a_{2u}e_{gy} + a_{1u}e_{gx})$$

$$|Q_y^0\rangle = \frac{1}{\sqrt{2}}(a_{2u}e_{gy} - a_{1u}e_{gx})$$

$$|B_x^0\rangle = \frac{1}{\sqrt{2}}(a_{2u}e_{gx} + a_{1u}e_{gy})$$

$$|Q_x^0\rangle = \frac{1}{\sqrt{2}}(a_{2u}e_{gx} - a_{1u}e_{gy})$$

and as a function of angle $\alpha$[1] that gives the deviation from equal mixing of the configurations of the B- and Q-band:

$$|B_y\rangle = \cos(\alpha)|B_y^0\rangle + \sin(\alpha)|Q_y^0\rangle$$

$$|Q_y\rangle = \cos(\alpha)|Q_y^0\rangle + \sin(\alpha)|B_y^0\rangle$$

$$|B_x\rangle = \cos(\alpha)|B_x^0\rangle + \sin(\alpha)|Q_x^0\rangle$$

$$|Q_x\rangle = \cos(\alpha)|Q_x^0\rangle + \sin(\alpha)|B_x^0\rangle$$

For $\alpha = 0°$, the intensity of the 0−0 transition is zero, and all intensity of the vibronic band is in the 0−1 transition. For weak vibronic coupling, all of the modes can be treated as individual vibronic progressions that can be summed to give the absorption spectrum and REP for the band. A 0−0 band will be observed for $\alpha > 10°$, that is, if there is a large deviation from the 50/50 states. For the Q-bands there is essentially no 0−0 transition, and we can conclude that $\alpha \approx 0°$.

The corresponding CI model for band III is

$$|B_y^0\rangle = \frac{1}{\sqrt{2}}(a_{2u}e_{gy} + a_{1u}e_{gx})$$

$$|CT_y^0\rangle = a_{2u}d_{yz}$$

$$|B_x^0\rangle = \frac{1}{\sqrt{2}}(a_{2u}e_{gx} + a_{1u}e_{gy})$$

$$|CT_x^0\rangle = a_{2u}d_{xz}$$

In this model, the splitting of the d$\pi$ orbitals into $d_{xz}$ and $d_{yz}$ has been assumed on the basis of the MCD data. The extent of mixing is given by the angle $\beta$ as indicated in the following equations.

$$|B_y\rangle = \cos(\beta)|B_y^0\rangle + \sin(\beta)|CT_y^0\rangle$$

$$|CT_y\rangle = \cos(\beta)|CT_y^0\rangle + \sin(\beta)|B_y^0\rangle$$

$$|B_x\rangle = \cos(\beta)|B_x^0\rangle + \sin(\beta)|CT_x^0\rangle$$

$$|CT_x\rangle = \cos(\beta)|CT_x^0\rangle + \sin(\beta)|B_x^0\rangle$$

It is an essential feature of the four orbital model that the $|G\rangle \rightarrow |B_x\rangle$ and $|G\rangle \rightarrow |B_y\rangle$ transitions are isoenergetic and that they have the same oscillator strength. Unlike the situation for the Soret $\pi-\pi^*$ transition, strong vibronic coupling in band III splits the d$\pi$ excited state. The nuclear coordinate dependence of the transition moment implies that the *x*- and *y*-transition moments are no longer equal. For weak mixing the angle $\beta = 0°$, and there is no 0−0 transition in the vibronically coupled band. However, for band III the most reasonable assumption is that $\beta \gg 0°$. This leads to an assignment for band III as the 0−0 transition. Spectral modeling based on Shelnutt's vibronic theory is presented in the Supporting Information.

A vibronic coupling model for band III provides a basis for exploring six observations that have not yet received an adequate explanation: (1) the small difference dipole moment measured by electroabsorption spectroscopy,[29] (2) the oblique angle for the transition moment of band III obtained from polarized single-crystal absorption spectra and electroabsorption spectroscopy,[23,29] (3) the B-term MCD signal observed for band III,[23] (4) the pseudo C-term MCD of the deoxy Soret band, (5) the presence of strong low-frequency $B_{1g}$ modes in the resonance Raman spectrum of the deoxy Soret band, and (6) the correlation between the conformationally dependent band shifts of the Soret band and band III. The electroabsorption spectrum of band III indicates that the difference dipole moment is small ($\Delta\mu_A$ = 0.9 ± 0.2 D) as compared to charge-transfer band I ($\Delta\mu_A$ = 3.5 ± 0.4 D) or even the Soret ($\Delta\mu_A$ = 2.6 ± 0.4 D) and Q-bands ($\Delta\mu_A = 3.3 \pm 0.4$ D).[29] The difference dipole moment is defined as the difference between the ground-state and excited-state dipole moments ($\Delta\mu_A = \mu_{excited} - \mu_{ground}$). The hypothesis of vibronic coupling for band III helps explain the small difference dipole moment observed in band III and, potentially, the relatively large difference dipole moment observed in the Soret band. For the latter, although it has long been suspected that the Soret band in deoxy myoglobin has some charge-transfer character,[35] there has never been direct evidence for a buried charge-transfer band. Further, the electroabsorption data show that there is no buried charge-transfer band. However, the difference dipole moment of the Soret band is larger than expected for a typical metalloporphyrin monomer with a center of symmetry,[29] indicating that vibronic mixing with a charge-transfer state may be present. Vibronic mixing gives charge-transfer character to the $\pi-\pi^*$ transition (Q and Soret) from band III, and in return band III can borrow oscillator strength from the strongly allowed $\pi-\pi^*$ transition.

The angle between the transition moment and the difference dipole moment was determined to be $\zeta_A = 54°$. This angle observed for band III is in agreement with single-crystal polarized absorption studies where it was found that the transition moment of band III has a significant *x*,*y* component

even though the charge transfer must occur along the *z* axis.[23] Although we do not perform a detailed analysis of the electroabsorption data, which can become quite complex if the coordinate dependence of the transition dipole is considered, the relative direction of the difference dipole moment and transition dipole is consistent with the vibronic coupling model. The direction of the transition moment must have a significant in-plane component both by orbital overlap considerations and due to mixing by the $B_{1g}$ modes that give rise to intensity borrowing from the Soret band. The 160 $cm^{-1}$ low-frequency mode that couples the CT excited state to the $\pi-\pi^*$ excited state is predominantly a rhombic in-plane distortion of the heme (perhaps best assigned as $\nu_{18}$) that has a small out-of-plane component.

The MCD of doubly degenerate states should be A-term as observed for the Soret band and Q-band of deoxy heme and other metalloporphyrins. However, the MCD spectrum of band III is B-term[23] and that of the deoxy myoglobin Soret band is C-term.[49,50] Both the B-term and the C-term signals imply symmetry breaking that lifts the degeneracy of the $d_{xz}/e_{gx}^*$ and $d_{yz}/e_{gy}^*$ orbitals.[48] A ground-state broken symmetry in the $d_\pi$ ($d_{xz}$, $d_{yz}$) orbitals in a high-spin $d^6$ configuration can lead to a nonaxially symmetric orbital occupation, such as $^2d_{xz}{}^1d_{xy}{}^1d_{yz}{}^1$-$d_{x^2-y^2}{}^1d_{z^2}$. The hypothesis of nonaxial symmetry for the heme iron, originally advanced to account for the B-term MCD signal, has been confirmed by Mössbauer spectroscopy.[51] The $d_\pi$ occupancy implies a Jahn−Teller splitting that will also couple to the excited-state $e_{g\pi^*}$ orbitals (but not the ground-state $a_{1u}$,$a_{2u}$ orbitals). The Jahn−Teller coupling due to the 160 $cm^{-1}$ $B_{1g}$ mode accounts for this coupling and the concomitant excited-state splitting. Further consideration of excited-state symmetry breaking is discussed in detail in a companion study of the MCD spectrum of deoxy heme.[48]

The frequencies of the Soret band and band III are both sensitive to protein conformational changes. Indeed, both the low-temperature photoproduct spectra and the room-temperature time-dependent spectra shifts are nearly identical for the Soret band and band III. The maximum shift is ∼140 $cm^{-1}$ at short times or in the photoproduct at cryogenic temperatures where protein relaxation cannot take place. Moreover, kinetic hole burning is observed in both band III and the Soret band.[12,20,21] The fact that the band shifts are correlated is puzzling at first since the nature of the electronic transitions is so different. The Soret band is the most intense electronic transition and is a strongly allowed $\pi-\pi^*$ transition ($\epsilon_{max} \approx 120\,000$ $M^{-1}$ $cm^{-1}$). Band III is the weakest electronic transition that has been studied ($\epsilon_{max} \approx 200$ $M^{-1}$ $cm^{-1}$). The resonant Raman data shown here present a clear explanation for the correlation of band III and the Soret band. The low-frequency $B_{1g}$ mode couples the Soret band and band III, but it also results in a Jahn−Teller split excited state for both absorption bands. Any ground-state geometry distortion that produces a rhombic symmetry change in the heme environment will cause a displacement of the nuclear coordinate along the lowest-frequency $B_{1g}$ mode. The principle that distortions occur along the lowest-frequency mode of a given symmetry has been demonstrated for out-of-plane distortions of hemes.[52] If we hypothesize that the lowest-frequency $B_{1g}$ mode is the 160 $cm^{-1}$ band seen in Figure 1 and that this mode couples the Soret band and band III excited states, the transition energy for both of these electronic transitions will be affected by distortion along this mode (see Figure 7). Thus, any symmetry breaking event can result in a shift that will be observed in both the Soret band and band III. Among other possibilities, the photolysis of CO produces such a change in conformation since the CO rests on the heme breaking the 4-fold symmetry of the ligated form.

The geometry of photolyzed Mb*CO has been studied by various spectroscopies and more recently by time-resolved X-ray crystallography[41] or cryogenic photoproduct crystallography.[42−45] Cryogenic photoproduct X-ray structures have given rise to a detailed picture of a docking site for the photolyzed CO molecule. The docking site involves CO resting on the heme ∼3.6 Å from the heme iron.[42] The transition moment of the CO is parallel to the heme plane. The fate of the CO at ambient temperature is not known in detail. However, there is a strong indication that the CO remains in the docking site, or in a similar site, for nearly 200 ns until it can escape from the globin.[46] Time-resolved infrared studies have shown that the CO molecule becomes localized in the docking site on the same time scale as the band III frequency shift.[3,45] As has been indicated previously, the Soret band shift is not correlated with factors that affect the proximal side of the heme. There is no correlation of the Soret band shift with the barrier to rebinding or changes in hydrogen bonding or even the covalent bond between the imidazole of proximal histidine (His93) and protein.[18] On the other hand, the Soret band shift is strongly affected by mutations in the distal pocket.[5] The band III Raman data presented in this study further indicate that conformational changes that result from CO photolysis do so from a change in the heme environment that has the effect of a rhombic distortion of the heme geometry.

The implications of the vibronic coupling of band III are far reaching. Numerous studies of the coupling of protein dynamics to ligand diffusion and rebinding in myoglobin have relied on studies of band III. Despite its small oscillator strength, band III is still the central observable for kinetic hole burning studies and ultrafast studies of protein relaxation.[3,4,9,11,12,14,15,18,20,25] The interpretation of these studies is crucial for the resolution of the more than 30 years of research into the coupling of conformation to function in myoglobin. The interpretation of the spectroscopy of band III in structural terms has often supported the central role of the heme iron in myoglobin dynamics. However, the data presented here suggest that electrostatic symmetry breaking or shifts in heme geometry and globin conformation parallel to the heme plane can play a key role in the band shifts observed following ligand photolysis. The band shifts at low temperature are correlated with a cryogenic X-ray crystal structure that shows the CO trapped in a pocket above the heme. This suggests that the CO itself and distal residues are at least part of the conformational change that gives rise to a time-dependent band shift. Band III and the Soret band track the time scale for this conformational change and thus provide information on how solvent viscosity, mutation, and temperature affect the protein relaxation around trapped CO. Although the heme iron, proximal histidine, and associated F-helix may also play a role, it is not the totally symmetric motions including heme doming and axial out-of-plane displacement of the heme iron that couple to band III. Rather, the

(51) Eicher, H.; Bade, D.; Parak, F. *J. Chem. Phys.* **1976**, *64*, 1446−1455.
(52) Shelnutt, J. A.; Song, X. Z.; Ma, J. G.; Jentzen, W. *Chem. Soc. Rev.* **1998**, *27*, 31−41.

motions that give rise to band shifts are those that couple to symmetry breaking modes of $B_{1g}$ symmetry. The data indicate an important role for vibronic effects in the studies of heme protein spectroscopy.

**Acknowledgment.** S.F. gratefully acknowledges a Los Alamos Director's Fellowship and NSF grant MCB-9874895. A.P.S. acknowledges funding from the Los Alamos LDRD program. We also thank Dr. R. Brian Dyer for experimental assistance.

**Supporting Information Available:** Raman excitation spectra, four orbital model, application to spectra, and Herzberg−Teller coupling (PDF). This material is available free of charge via the Internet at http://pubs.acs.org.

JA0172722